Hygrocins A and B, Naphthoquinone Macrolides from *Streptomyces hygroscopicus*

Ping Cai,*,† Fangming Kong,‡ Mark E. Ruppen,† Greg Glasier,† and Guy T. Carter‡

Chemical and Pharmaceutical Development, and Chemical and Screening Sciences, Wyeth Research, 401 N. Middletown Road, Pearl River, New York 10965

Received July 27, 2005

Two new naphthoquinone macrolides, hygrocins A (**1**) and B (**2**), were isolated from the fermentation broth of *Streptomyces hygroscopicus*. Hygrocin A is not stable due to the presence of an active methylene group (C-22), which undergoes intramolecular aldol condensation with the quinone ring to yield a γ-lactam derivative, **6**. Its structural elucidation was achieved by chemical conversion to **3**, an unusual diazomethane derivative, and confirmed by its alkaline hydrolysis product **4**, hydrogenation derivative **5**, and "degradation" product **6**. The structure of hygrocin B was determined by combined chemical and spectroscopic methods.

Streptomyces hygroscopicus ATCC25293 is well-known for producing the immunosuppressive agent rapamycin, which is being used in combination with cyclosporine for treatment of allograft rejection.[1] In addition, several other antibacterial secondary metabolites, including nigericin,[2] elaiophylin,[3] and hexaenes,[4] have also been isolated from this strain. In the rapamycin purification process, we found that some bright yellow pigments cocrystallized with rapamycin. These yellow pigments showed unique UV spectra, which did not resemble any other frequently encountered metabolites from *Streptomyces hygroscopicus* ATCC25293. A UV-guided isolation was conducted, which led to the discovery of two new naphthoquinone macrolides, hygrocins A (**1**) and B (**2**). This paper describes the isolation, structure elucidation, and chemistry of these compounds, including the preparation and structure elucidation of their derivatives **3**, **4**, **5**, **6**, **7**, and **8**.

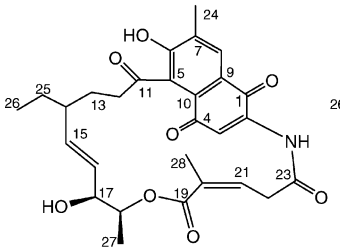

Hygrocin A (**1**)

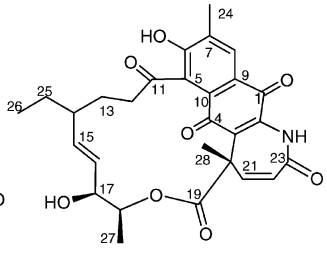

Hygrocin B (**2**)

Results and Discussion

The mycelia cakes from 10 L fermentation broth of *Streptomyces hygroscopicus* ATCC25293 were collected and extracted with acetone. After the solvent was removed under vacuum, Et_2O was added to the residue to precipitate unwanted solids, and the filtrate was collected and concentrated to obtain the crude oil containing hygrocins A and B. The yellow oil was then subjected to separation by reversed-phase preparative HPLC to yield pure hygrocins A (**1**, 200 mg) and B (**2**, 98 mg) as yellow powders.

The molecular weight of hygrocin A (**1**) was determined to be 509 by both positive and negative electrospray ionization mass spectroscopy (EIMS), and the molecular formula was found to be $C_{28}H_{31}NO_8$ by high-resolution FT-ICR mass. A strong absorption band at 1663 cm^{-1} in the IR spectrum and absorption maxima at 275 and 316 nm in the UV spectrum of **1** suggested the presence of a conjugated quinone system. Hygrocin A was soluble in MeOH and DMSO, but showed poor solubility in H_2O and other organic solvents. It was very unstable under acidic and basic conditions and slowly decomposed in MeOH and DMSO. Considering DMSO was able to dissolve any derivatives of **1**, DMSO-d_6 was finally selected as the NMR solvent. The ^1H NMR spectrum of **1** showed the presence of three methyl groups (δ 0.84, d; 1.88, s; 2.31, s), one ethyl group (δ 0.77, t; 1.24, q), two oxygenated methine protons (δ 3.88, bd; 4.64, bq), three olefinic protons (δ 5.03, 5.27, 6.36), and two aromatic protons (δ 7.10, s; 7.67, s, Table 1). The remaining resonances were poorly resolved and shifted during 2D-NMR data collection. The ^{13}C NMR spectrum of **1** showed the presence of four methyl carbons (δ 19.8, 16.7, 16.3, and 11.6), 12 aromatic or double-bond carbons (δ 156.9, 142.0, 136.5, 132.1, 131.6, 131.0, 130.9, 129.8, 128.8, 126.9, 122.0, and 115.8), and five carbonyl carbons (δ 204.2, 184.8, 179.2, 172.2, and 167.0). The remaining carbon signals in the range δ 27−75 were too broad to be assigned and are labeled with asterisks in Table 2. Although the carbon signals at δ 184.8 and 179.2 were indicative of quinone carbonyls and evidenced the presence of a quinone moiety, it was difficult to complete the structure assignment of **1** solely on the basis of NMR data. The structure of **1** was finally deduced from its stable diazomethane derivative **3** (Figure 1) and confirmed by its base hydrolysis product **4** (Figure 1), hydrogenation derivative **5** (Figure 1), and "degradation" product **6** (Figure 1).

Treating **1** with freshly prepared CH_2N_2 afforded a major adduct, **3**, with pseudomolecular ion at *m/z* 550 $[M - H]^-$, 42 mass units higher than that of **1**. This result suggested that three CH_2 units had been inserted into the original molecule. This derivative showed a maximum UV absorption at 267 nm and a shoulder at 302 nm. The disappearance of the 316 nm absorption band in the starting compound **1** implied that the original quinone chromophore had been disrupted, which was supported by the NMR data of **3**. For compound **3**, only one oxygenated methyl proton singlet at δ 3.90 was observed in the ^1H NMR spectrum. This methoxy proton signal showed HMBC correlation to

* To whom correspondence should be addressed. Tel: 845-602-5261. Fax: 845-602-5592. E-mail: caip@wyeth.com.
† Chemical and Pharmaceutical Development.
‡ Chemical and Screening Sciences.

10.1021/np050272l CCC: $30.25
Published on Web 12/02/2005

Table 1. ^{1}H NMR Data of Hygrocin A (**1**) and Derivatives **3**, **4**, **5**, and **6** in DMSO-d_6

position	1	3	4	5	6
3	7.10 (s)		5.64 (s)	7.47 (s)	5.66 (s)
8	7.67 (s)	7.71 (s)	7.75 (s)	7.87 (s)	7.24 (s)
12	2.40 (m)	1.85/2.33 (m)	2.50 (m)	2.42/2.63 (m)	2.71/2.44 (m)
13	1.60/1.81 (m)[a]	1.51/1.72 (m)	1.56/1.78 (m)	1.12/1.26 (m)	1.33/1.27 (m)
14	1.45 (br)[a]	1.70 (m)	1.98 (m)	0.54 (m)	1.26 (m)
15	5.27 (dd, 16.2, 7.5)	5.60 (dd, 16.2, 7.8)	5.38 (overlap with H-16)	0.71/1.32 (m)	5.15 (dd, 16.2, 7.6)
16	5.03 (dd,16.2, 3.5)	5.41 (dd, 16.2, 3.1)	5.29 (overlap with H-15)	0.41/0.89 (m)	3.95 (dd, 16.2, 3.2)
17	3.88 (bd, 3.5)	4.11 (bd, 3.1)	3.67 (bd, 4.0)	3.08 (m)	3.75 (bd, 3.0)
18	4.64 (bq, 6.8)	4.95 (bq, 6.8)	3.40 (bq, 6.8)	4.53 (m)	4.72 (dq, 6.8)
20				2.26 (m)	
21	6.36 (br)	2.43 (bd, 6.8)		1.72 (m)	6.46 (d, 8.0)
22	3.57 (bd)[a]	2.26/2.49 (m)		2.30/2.85 (m)	4.36 (d, 8.0)
24	2.31 (s)	2.30 (s)	2.27 (s)	2.32 (s)	2.13 (s)
25	1.24/1.27(m)[a]	1.35 (m)	1.24/1.40 (m)	1.01/1.21(m)	0.82/1.36 (m)
26	0.77 (bt, 6.0)	0.83 (t, 7.0)	0.83 (t, 7.2)	0.68 (bt, 6.5)	0.55 (t, 6.8)
27	0.84 (bd, 6.5)	1.19 (d, 6.8)	0.91 (d, 6.8)	0.89 (d, 6.9)	0.89 (d, 6.8)
28	1.88 (s)	0.78 (s)		1.06 (d, 7.0)	2.12 (s)
OH	9.42 (br)	6.38 (s)	7.15 (br)	4.86 (s)	6.73 (s)
	9.60 (br)	7.81 (s)	9.01 (s)	7.15 (br)	9.02 (s)
NH	10.23 (br)	8.15 (s)	11.31 (br)	9.81 (s)	11.03 (s)
OCH_3		3.90 (s)			
cyclopropane		0.06/0.45 (m)			
		0.52/1.10 (m)			

[a]These signals are very broad.

Table 2. ^{13}C NMR Data of Hygrocin A (**1**) and Derivatives **3**, **4**, **5**, and **6** in DMSO-d_6

carbon position	1	3	4	5	6
1	179.2 (s)	194.1 (s)	180.1 (s)	179.3 (s)	71.8 (s)
2	142.0 (s)	74.5 (s)	150.4 (s)	141.5 (s)	162.3 (s)
3	115.8 (d)	41.1 (s)	101.5 (d)	115.0 (d)	102.5 (s)
4	184.8 (s)	92.3 (s)	181.8 (s)	185.7 (s)	182.9 (s)
5	122.0 (s)	120.7 (s)	122.3 (s)	122.0 (s)	128.3 (s)
6	156.9 (s)	158.2 (s)	156.5 (s)	157.6 (s)	151.6 9s)
7	130.9 (s)	132.5 (s)	130.3 (s)	131.4 (s)	130.3 (s)
8	129.8 (d)	130.0 (d)	129.1 (d)	129.7 (d)	128.9 (d)
9	130.9 (s)	131.4 (s)	128.9 (s)	128.1 (s)	132.6 (s)
10	132.1 (s)	151.1 (s)	130.3 (s)	129.0 (s)	130.5 (s)
11	204.2 (s)	111.5 (s)	204.2 (s)	204.7 (s)	206.5 (s)
12	40.1 (t)[a]	37.9 (t)	40.8 (t)	39.5 (t)	38.9 (t)
13	28.5 (t)[a]	29.2 (t)	28.3 (t)	27.7 (t)	29.9 (t)
14	42.5 (d)[a]	41.3 (d)	43.0 (d)	38.1 (d)	44.0 (d)
15	136.5 (d)	132.8 (d)	134.5 (d)	28.7 (t)	134.8 (d)
16	128.8 (d)	131.6 (d)	130.7 (d)	28.3 (t)	126.9 (d)
17	73.1 (d)[a]	71.2 (d)	75.6 (d)	71.1 (d)	68.9(d)
18	74.4 (d)	72.6 (d)	69.6 (d)	73.4 (d)	73.2(d)
19	167.0 (s)	170.2 (s)		175.4(s)	166.2 (s)
20	126.9 (s)	54.9 (s)		36.4 (d)	134.3 (s)
21	131.6 (d)	49.7 (d)		30.4 (t)	130.3 (d)
22	36.5 (t)[a]	32.8 (t)		34.7 (t)	53.3 (d)
23	172.2 (s)	176.4 (s)		174.2 (s)	175.0 (s)
24	16.7 (q)	16.0 (q)	16.4 (q)	16.9 (q)	16.8 (q)
25	27.5 (t)	29.7 (t)	27.4 (t)	25.5 (t)	25.3 (t)
26	11.6 (q)	11.9 (q)	11.5 (q)	10.6 (q)	12.6 (q)
27	16.3 (q)	16.4 (q)	18.4 (q)	13.3 (q)	13.4 (q)
28	19.8 (q)	23.4 (q)		16.8 (q)	21.5 (q)
OCH_3		61.1 (q)			
cyclopropane		0.5 (t)			
		7.7 (t)			

[a] These signals are very weak.

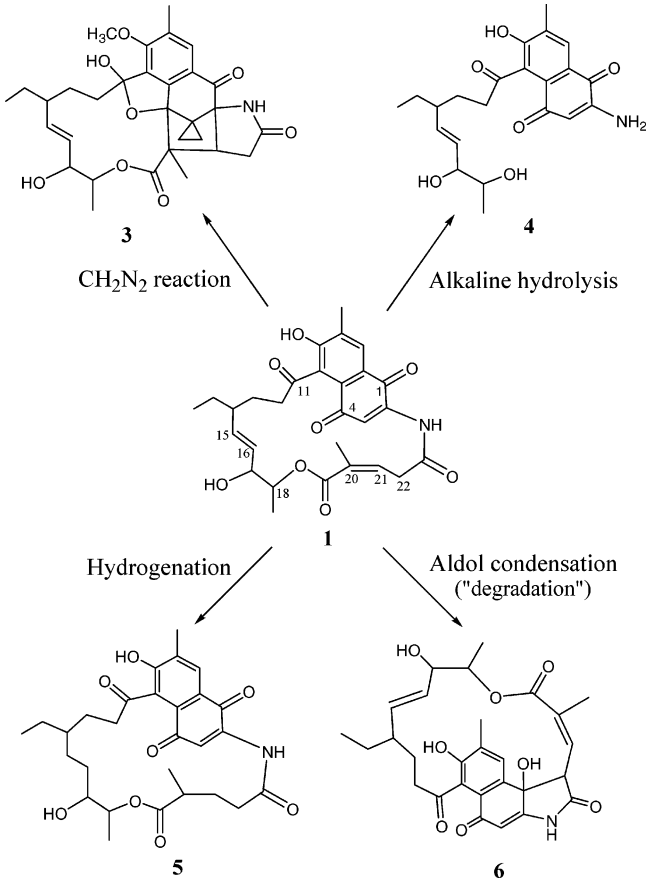

Figure 1. Hygrocin A (**1**) and its derivatives **3**, **4**, **5**, and **6**.

an aromatic carbon at δ 158.2 (C-6), suggesting the presence of a phenolic hydroxy group in **1**. The ^{1}H NMR spectrum of **3** displayed only one aromatic proton (δ 7.71) instead of two aromatic protons in **1**. This aromatic proton showed three strong HMBC correlations to carbons at δ 151.1, 158.2, and 194.1 and one weak correlation to the carbon at δ 120.7. These signals were assigned to C-10, C-6, C-1, and C-5, respectively, revealing a possible partial structure **3a** (Figure 2). The four-bond coupling to C-5 was confirmed by its HMBC correlations to the hemiacetal hydroxy proton and H-12 (vide infra). The appearance of two pairs of upfield methylene proton signals in the range δ 0.06 to 1.10 indicated the presence of a cyclopropane ring. The HMBC correlations from the cyclopropane methylene protons to three quaternary carbons at δ 41.1 (C-3), 74.5 (C-2), and 92.3 (C-4) suggested a substructure **3b** (Figure 2), in which the carbons at δ 92.3 and 74.5 must be connected with either oxygen or nitrogen atoms to account for their chemical shifts. The HMBC spectra of **3** also showed long-range couplings from the most upfield methyl

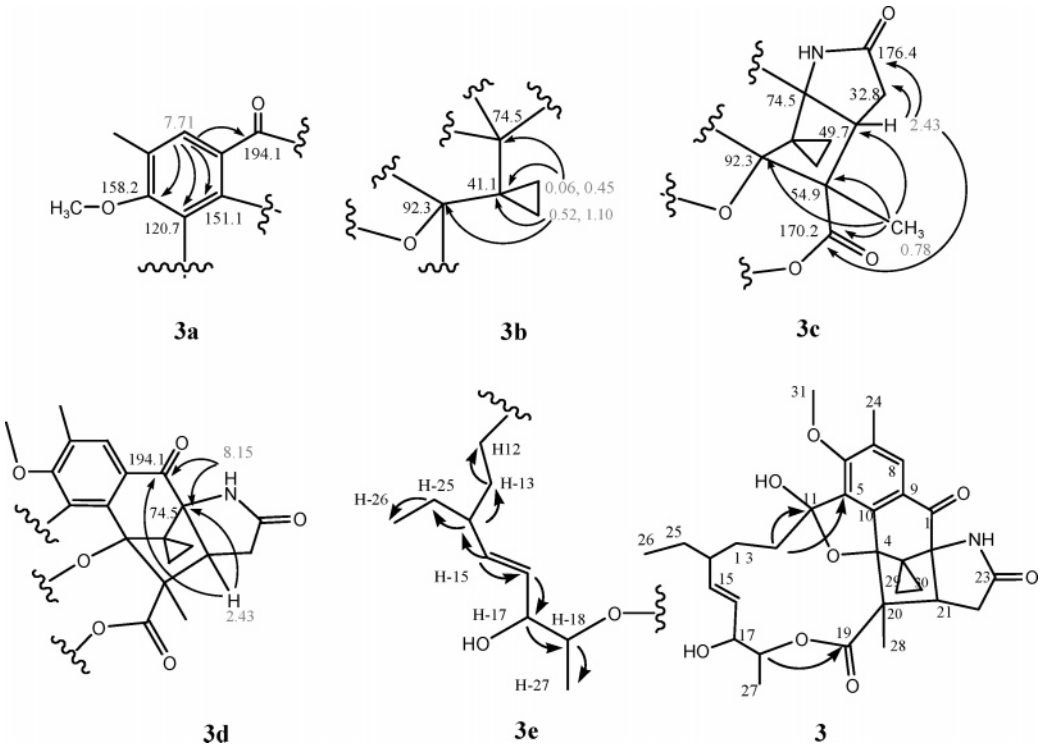

Figure 2. Structure **3** and its partial structures with key HMBC correlations (**3a**, **3b**, **3c**, and **3d**) and $^1H-^1H$ correlations (**3e**).

proton (δ 0.78, H-28) to a carbonyl carbon at δ 170.2 (C-19), methine carbon at δ 49.7 (C-21), and quaternary carbons at δ 92.3 (C-4) and 54.9 (C-20). Combined with the observation of long-range correlations from the methine proton at δ 2.43 (H-21) to the quaternary carbon at δ 74.5 (C-2), the methylene carbon at δ 32.8 (C-22), and the carbonyl carbons at δ 170.2 (C-19) and 176.4 (C-23), the partial structure could be extended from **3b** to **3c** (Figure 2). The long-range correlations of the same methine proton (H-21) and the amine proton (δ 8.15) to the carbonyl carbon of **3a** at δ 194.1 (C-1) and the quaternary carbon of **3c** at δ 74.5 (C-2) indicated the connectivity of **3c** to **3a** and established the partial structure **3d** (Figure 2). The substructure **3e**, which involved almost all the remaining protons, was assembled by analysis of the $^1H/^1H$ correlations observed from the COSY spectrum. Starting from two coupled olefinic protons at δ 5.41 (H-16) and 5.60 (H-15), the $^1H/^1H$ correlations could be traced to two methine protons at δ 4.11 (H-17) and 1.70 (H-14), respectively. The downfield methine proton also coupled to an oxygenated methine proton at δ 4.95 (H-18), which in turn correlated to a methyl doublet at δ 1.19 (H-27). The upfield methine proton (H-14) showed correlation to two methylene protons at δ 1.35 (q, H-25) and 1.51 (m, H-13), which correlated to a methyl triplet at δ 0.83 (H-26) and another set of methylene protons at δ 2.33 (H-12), respectively. Thus, the substructure **3e** was delineated (Figure 2). The HMBC correlation from H-18 at δ 4.95 to the carbonyl carbon at δ 170.2 (C-19) and the correlation from H-12 at δ 2.33 to the quaternary carbon at δ 111.5 (C-11) and aromatic carbon at δ 120.7 (C-5) connected the substructure **3d** and **3e** (Figure 2). The chemical shift of the quaternary carbon at δ 111.5 (C-11) suggested that it was bonded to two oxygen atoms, probably in a five-membered hemiacetal ring as required by the unsaturation degree of the molecular formula. The formation of this hemiacetal moiety was proved by the HMBC correlations of its hydroxy proton at δ 6.38 to C-5, C-11, and C-12. Extensive $^1H/^1H$, $^1H/^{13}C$ correlation studies and chemical shift analysis established the structure **3** for the major diazomethane derivative (Figure 2).

Since the signals assigned to the cyclopropane ring were not observed in the NMR spectra of the starting compound **1**, it must have resulted from the diazomethane addition reaction. To verify this, **1** was treated with ^{13}C-labeled diazomethane to generate the ^{13}C-labeled product. The ^{13}C NMR spectrum of this product was identical to that of **3** except that the signals assigned to the methoxy group (δ 61.2) and cyclopropane methylene carbons (δ 0.5 and 7.7) were much stronger. In addition, the cyclopropane methylene carbons appeared as doublets due to one-bond $^{13}C/^{13}C$ coupling ($J \approx 10$ Hz). These results clearly indicated that these three carbons came from the ^{13}C-labeled diazomethane and supported the proposed structure **3** (Figure 2).

On the basis of the diazomethane derivative structure, a naphthoquinone macrolide structure is proposed for hygrocin A (**1**, Figure 3), which incorporated the features deduced from the UV and NMR data of **1**. When reacting with diazomethane, in addition to phenol methylation, **1** probably also undergoes a CH_2 insertion and a Michael addition followed by a second CH_2 insertion and intramolecular cyclization to produce compound **3**.[5] Figure 3 depicts a possible mechanism for conversion of **1** to **3** upon reaction with diazomethane. These sequential reactions disrupted the original naphthoquinone conjugation system of **1**. As a consequence, the UV absorption band at 316 nm disappeared and only one of the original two quinone carbonyl carbons was observed (δ 194.1) in the ^{13}C NMR spectrum of **3**.

According to the deduced structure, hygrocin A (**1**) contains one ester bond and one amide bond, which should be easily hydrolyzed to form a stable naphthoquinone with an opened side chain. To confirm the proposed structure of **1**, especially the naphthoquinone skeleton, an alkaline hydrolysis was conducted and the major hydrolysis product **4** was isolated. Compound **4** gave a molecular ion of *m/z*

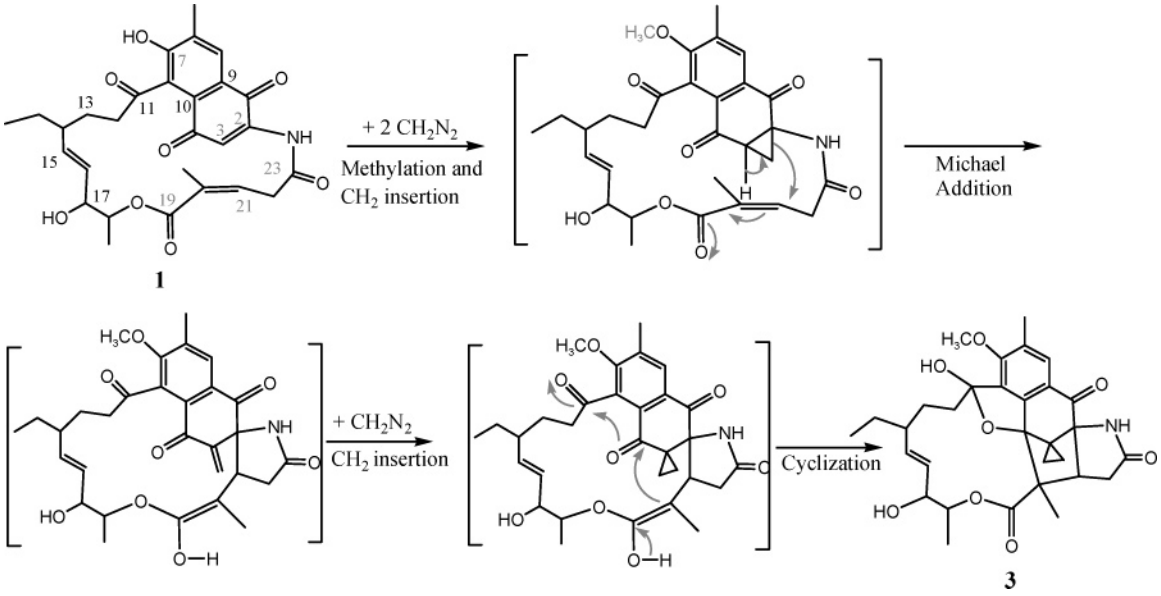

Figure 3. Proposed mechanism for conversion of **1** to **3**.

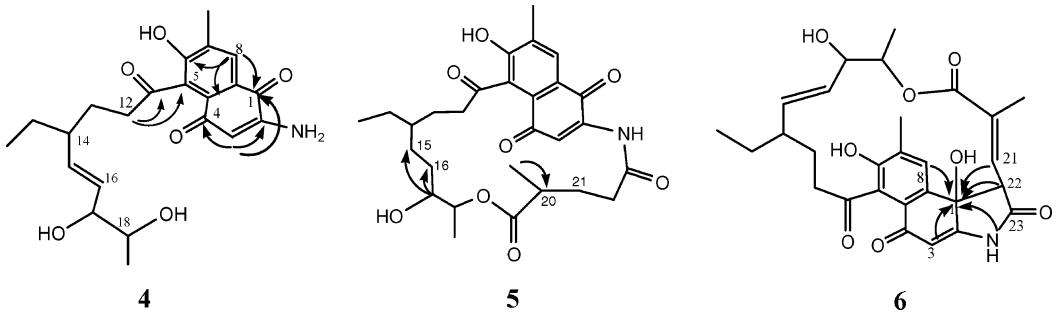

Figure 4. Alkaline hydrolytic product **4**, hydrogenation product **5**, and degradation product **6** with key HMBC correlations.

400 in the EIMS spectrum and showed the same UV absorption as compound **1**. These data were consistent with the expected structure after cleavage of the ester and amide bonds of **1**. Like compound **1**, this hydrolytic product displayed two quinone carbonyl carbons (δ 180.1, C-1; δ 181.8, C-4) in the ^{13}C NMR spectrum and two aromatic protons (δ 5.64, H-3; δ 7.75, H-8) in the ^{1}H NMR spectrum. In the HMBC spectrum, the downfield aromatic proton (H-8) showed long-range correlations to the carbonyl carbon at δ 180.1 (C-1) and aromatic carbons at δ 156.5 (C-6) and 130.3 (C-10), while the upfield aromatic proton (H-3) displayed long-range coupling with both carbonyl carbons at δ 180.1 (C-1) and 181.8 (C-4) and aromatic carbons at δ 130.3 (C-10) and 150.5 (C-2). These observations, depicted in **4** of Figure 4, strongly supported the naphthoquinone skeleton of **1**. Like compound **3**, the side chain proton spin system from H-12 to H-18 was easily delineated by the COSY spectrum of **4**. This spin system connecting to the aromatic carbon C-5 through the C-11 carbonyl group was indicated by the long-range correlations from H-12 (δ 2.50) to C-5 (δ 122.3) and the carbonyl carbon C-11 (δ 204.2) in the HMBC spectrum. On the basis of NMR studies, the structure of the hydrolysis product was unambiguously assigned as **4** (Figure 4), which confirmed the proposed naphthoquinone structure of **1**.

When **1** was treated with H_2 in the presence of Pd/C, the hydrogenated product **5** was obtained. This product showed the same UV spectrum as **1** and displayed molecular ions at *m/z* 512 in the negative EIMS, 4 mass units more than that of **1**, suggesting that two double bonds had been hydrogenated. The ^{1}H and ^{13}C NMR spectra of **5** resembled those of **1** and **4** except for the side chain signals (Tables 1 and 2). Instead of double-bond resonances, compound **5** exhibited additional methylene signals (^{1}H/^{13}C: δ 0.71, 1.32/28.7; 0.41, 0.89/28.3; 1.72/30.4) and a methine signal (^{1}H/^{13}C: δ 2.26/36.4), which agreed with the EIMS result. In the HMBC spectrum, the long-range correlations from the carbinol proton at δ 3.08 (H-17) to the methylene carbons at δ 28.7 and 28.3 and from the methyl proton doublet at δ 1.06 (H-28) to the methine carbon C-20 at δ 36.4 clearly indicated the hydrogenated double-bond positions at C-15/C-16 and C-20/C-21 (**5** of Figure 4).

As mentioned above, compound **1** was not stable and easily converted to two more polar "degradation" products in MeOH or DMSO. Both "degradation" products showed the same molecular weight as **1**, but different UV absorption spectra. The "degradation" products displayed UV absorption bands at 275 and 306 nm instead of at 275 and 316 nm in **1**, indicating a change in the naphthoquinone chromophore. The NMR data of the isolated major "degradation" product **6** provided more evidence for the structural change. Compared to compound **1** and the base hydrolysis product **4**, the "degradation" product gave similar ^{1}H NMR and ^{13}C NMR spectra except for the quinone signals (Tables 1 and 2). The ^{13}C NMR of **6** showed only one of the original two quinone carbonyl carbons at δ 182.9 (C-4), but one more oxygenated quaternary carbon at δ 71.8. In the HMBC experiment, this oxygenated quaternary carbon showed strong long-range coupling to both aromatic protons (H-3 and H-8), whereas in compounds **1** and **4**, H-3 and H-8 showed HMBC correlations to the quinone carbonyl carbon C-1. This implied that the quaternary carbon in **6** had replaced the original C-1

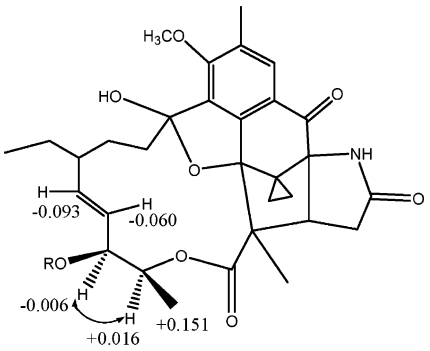

3s: R= (*S*)-MTPA
3r: R= (*R*)-MTPA

Figure 5. $\Delta\delta$ values $[\delta_{(S)} - \delta_{(R)}]$ for MTPA esters of **3**, and selected NOESY correlations.

quinone carbonyl carbon. This was supported by the observation of a long-range correlation between the NH proton (δ 11.03) and this carbon (δ 71.8) in the HMBC spectrum. The additional long-range correlations from the methine proton at δ 4.36 (H-22) and the double-bond proton at δ 6.46 (H-21) to the same quaternary carbon (δ 71.8) required a five-membered ring that included C-1, C-2, −NH−, C-23, and C-22, thus establishing the structure of **6** (Figure 4). This "degradation" product may have resulted from an intramolecular cyclization via Aldol type condensation between the active methylene (C-22) and the quinone carbonyl carbon (C-1).

The configuration of the double bonds in **1** was assigned as 15*E* and 20*Z* on the basis of the coupling constant of $J_{H15/H16} = 16.2$ Hz and the relative downfield chemical shift of the allylic methyl carbon (C-28: δ 19.8). The relative configurations of C-17and C-18 were deduced by $^1H-^1H$ coupling constants and NOESY correlations of **1** and **3**. The very small vicinal coupling constant of $J_{H17/H18} < 1$ Hz in both **1** and **3** indicated that the dihedral angle of these two protons was about 90°. The strong NOEs between H-17 and H-18 but not between H-17 and the methyl protons H-27 of **3** suggested that H-17 was in the opposite orientation from this methyl group (Figure 5). The absolute configuration of C-17 was assigned by application of modified Mosher's method.[6] Since **1** was not stable, Mosher's MTPA esters were prepared by treating **3** with (*R*)- and (*S*)-MTPACl in anhydrous pyridine, to yield the corresponding (*S*)- and (*R*)-MTPA esters **3s** and **3r**, respectively. On the basis of the $\Delta\delta$ $[\delta_{(S)} - \delta_{(R)}]$ values of the Mosher's MTPA esters shown in Figure 5, the C-17 *S* configuration was established for **3**. Since the C-17 configuration was not affected in the conversion of **1** to **3**, the C-17 configuration of **1** should also be *S*.

Hygrocin B (**2**) has the molecular formula $C_{28}H_{29}NO_8$ as derived from positive HRFT-ICR mass, indicating the presence of one more unsaturation site than **1**. Like compound **1**, the ^{13}C NMR and HMQC spectra of **2** revealed the presence of five carbonyl carbons (δ 208.7, 184.9, 179.7, 174.3, and 166.3), four methyl carbons (δ 25.8, 16.9, 16.6, and 12.1), 12 aromatic or double-bond carbons (δ 159.2, 146.2, 137.1, 136.8, 133.1, 132.6, 131.8, 131.7, 130.2, 124.6, 123.3, and 123.2), and three methine carbons (δ 76.7, 74.8, and 44.5). However, while **1** showed the presence of four methylene carbons (C-12, C-13, C-22, and C-25), **2** displayed three methylene carbons (δ 41.5, 29.6, and 28.3) and one quaternary carbon (δ 52.4) in the ^{13}C NMR spectrum (Table 3). The ^1H NMR of **2** showed the presence of the downfield aromatic proton (δ 7.91, H-8), but the upfield aromatic proton was absent as compared to **1**. Besides the H-15 (δ 5.28) and H-16 (δ 5.24) double-bond protons, **2** also displayed another pair of olefinic doublets at δ 6.18 (H-21) and 6.02 (H-22). H-22 showed a strong long-range correlation to the amide carbonyl carbon at δ 166.3 (C-23), and H-21 showed long-range correlations to both the amide carbonyl carbon (C-23) and the ester carbonyl carbon at δ 174.3 (C-19, Figure 6). These double-bond protons, as well as the methyl protons at δ 1.56 (H-28), also showed long-range couplings to the quaternary carbon C-20 at δ 52.5. In the HMBC spectrum, the long-range correlations from the same H-28 methyl proton to the C-19 ester carbonyl carbon and the C-21 and C-22 double-bond carbons, as well as to one of the aromatic carbons C-3 (δ 131.7), were also detected. These observations, combined with the long-range correlations from H-18 (δ 4.86) to the ester carbonyl carbon, revealed the structure **2** for hygrocin B (Figure 6).

Table 3. ^1H and ^{13}C NMR Data of Hygrocin B (**2**) and Derivative **7** in CD_3OD

	2		**7**	
position	δ_C	δ_H	δ_C	δ_H
1	179.7 (s)		180.1 (s)	
2	137.1 (s)		138.4 (s)	
3	131.7 (s)		137.2 (s)	
4	184.9 (s)		184.5 (s)	
5	123.3 (s)		124.8 (s)	
6	159.2 (s)		161.5 (s)	
7	133.2 (s)		140.5 (s)	
8	131.8 (d)	7.91 (s)	129.9 (d)	8.11 (s)
9	130.2 (s)		132.1 (s)	
10	126.4 (s)		127.3 (s)	
11	208.7 (s)		207.6 (s)	
12	41.5 (t)	2.73 (dd, 7.8, 1.6)	41.6 (t)	2.72 (dd, 7.8, 1.6)
13	28.3 (t)	1.53/2.03 (m)	28.3 (t)	1.51/1.97 (m)
14	44.5 (d)	1.51 (m)	44.5 (d)	1.47 (m)
15	136.8 (d)	5.28 (dd, 16.0, 6.1)	136.6 (d)	5.28 (dd, 16.0, 6.1)
16	132.6 (d)	5.24 (dd, 16.0, 6.1)	132.5 (d)	5.24 (dd, 16.0, 6.1)
17	74.8 (d)	3.98 (bd, 3.5)	74.6 (d)	3.97 (bd, 3.5)
18	76.7 (d)	4.86 (bq, 6.8)	76.5 (d)	4.87 (bq, 6.8)
19	174.3 (s)		174.2 (s)	
20	52.4 (s)		52.5 (s)	
21	146.2 (d)	6.18 (d, 12.0)	146.1 (d)	6.17 (d, 12.0)
22	123.2 (d)	6.02 (d, 12.0)	123.1 (d)	6.03 (d, 12.0)
23	166.3 (s)		166.2 (s)	
24	16.9 (q)	2.35 (s)	16.7 (q)	2.44 (s)
25	29.6 (t)	1.32 (m)	29.6 (t)	1.32 (m)
26	12.1 (q)	0.80 (t, 6.5)	12.6 (q)	0.79 (t, 6.5)
27	16.6 (q)	1.29 (d, 6.8)	16.5 (q)	1.29 (d, 6.8)
28	25.8 (q)	1.56 (s)	25.8 (q)	1.54 (s)
OCH_3			63.2 (q)	3.77 (s)

According to structure **2**, hygrocin B does not contain the active methylene group (C-22 in **1**) between the amide and the ester bonds, making it much more stable than **1** in MeOH and other solvents. For the same reason, treating **2** with diazomethane yielded only phenolic methylation product **7**. No CH_2 insertion or intramolecular cyclization occurred for **2**. When hygrocin B was treated with 1 N NaOH, product **8** was obtained. In the negative EIMS, this product gave a molecular ion at *m/z* 524 and the fragment ions at *m/z* 480 and 437 due to allylic cleavage followed by the loss of NH═C═O (**8**, Figure 6), providing further support for the assigned structure of **2**.

The configuration of the double bonds in **2** was assigned as 15*E* and 21*Z* on the basis of olefinic proton coupling constants ($J_{H15/H16} = 16.0$ Hz, $J_{H21/H22} = 12.0$ Hz). The relative configuration of C-17 and C-18 was identical to that of **1**, as confirmed by the analysis of NOESY correlations and coupling constant data. The strong NOEs between the C-18 and C-20 methyl protons observed in both 1D-NOE and 2D-NOESY experiments indicated that these two methyl groups were in the same orientation. By the

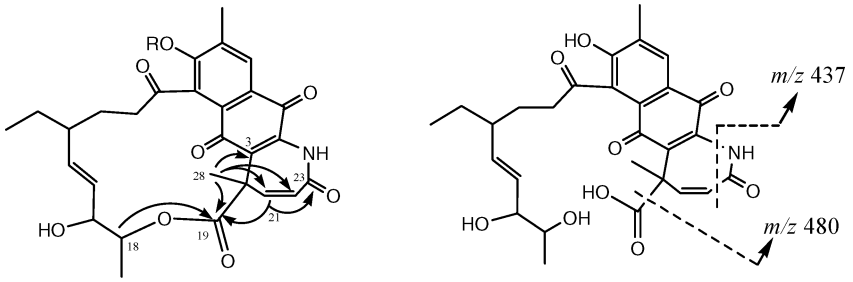

2: R= H
7: R= CH_3

8

Figure 6. Structures of hygrocin B (**2**) with key HMBC correlations, methylation product **7**, and alkaline hydrolysis product **8** with MS/MS fragmentation assignments.

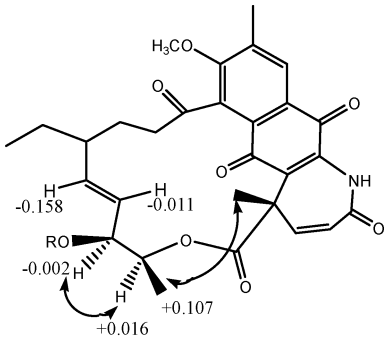

7s: R= (*S*)-MTPA
7r: R= (*R*)-MTPA

Figure 7. $\Delta\delta$ values [$\delta_{(S)} - \delta_{(R)}$] for MTPA esters of **7**, and selected NOESY correlations.

modified Mosher's method, the absolute configuration of C-17 of **2** was assigned as *S* on the basis of the $\Delta\delta$ [$\delta_{(S)} - \delta_{(R)}$] values of **7s** and **7r** demonstrated in Figure 7.

On the basis of spectroscopic data and chemical reactions, hygrocins A and B were identified as new ansamycin macrolides, a class of interesting natural products consisting of a naphthoquinone or naphthohydroquinone ring and an aliphatic bridge linking two nonadjacent positions of the aromatic rings. Well-known antimicrobial agents, such as streptovaricins,[7] naphthomycins,[8,9] and rifamycins,[10,11] all belong to this group. However, all the known ansamycins have much longer aliphatic chains than hygrocins A and B. For example, streptovaricins and rifamycins have a bridge chain of 17 carbons, and naphthomycins have a bridge chain of 23 carbons. Hygrocins A and B are the ansamycins with the shortest bridge ring (13 carbons) thus far isolated, which might account for their much weaker biological activity as compared with the above-mentioned known ansamycins (Table 4).[12]

Experimental Section

General Experimental Procedures. Optical rotations (25 °C, 10 cm cell) were measured on a Jasco P-1020 polarimeter. IR spectra were recorded on a Perkin-Elmer RX1 FT-IR spectrophotometer. UV spectra were obtained on a Shimadzu UV-2501PC spectrophotometer. ^{1}H and ^{13}C NMR spectra were acquired on a Bruker 400 AMX spectrometer. The chemical shifts (δ) are given in ppm and were referenced to the solvent signal: δ H/C 2.49/39.5 and δ H/C 3.30/49.0 for DMSO-d_6 and CD_3OD, respectively. LC-MS analysis was performed using an Agilent 1100 HPLC coupled with a MSD 1100 mass spectrometer. EIMS data were acquired at unit resolution from *m/z* 150 to 1000. The high-resolution mass measurement was conducted using a Bruker Apex-II 9.4 T electrospray FT-ICR mass spectrometer. Analytical HPLC was conducted on a Waters Alliance HPLC system equipped with a Waters model 996 photodiode array detector. The isolation of hygrocins A and B as well as their derivatives was accomplished using a Waters Delta 4000 Prep-HPLC system.

Table 4. Antimicrobial Activity of Hygrocin A and Hygrocin B in Comparison to Rifamycin S

	MIC (μg/mL)		
organism	hygrocin A[12a]	hygrocin B[12a]	rifamycin S[12b,c]
Staphylococcus aureus 2999	128	128	0.01
Streptococcus pneumoniae	16	128	0.1
Streptococcus faecalis 1362/3	128	128	16
Haemophilus influenzae	128	128	0.01
Neisseria gonorrheae	64	128	0.1
Escherichia coli 1074	128	128	128
Candida albicans	128	128	
Aspergillus fumigatus	16	32	
Aspergillus niger	32	64	

Fermentation. *Streptomyces hygroscopicus* ATCC25293 was cultivated in liquid culture, e.g., tryptic soy broth, at 30 °C and 200 rpm for 48 h. This seed culture was inoculated into fermentation medium containing 2% Pharmamedia, 0.5% yeast extract, 2% glycerol, 0.1% K_2HPO_4, 0.1% KH_2PO_4, 0.5% NaCl, and 2% D-glucose in 250 mL Erlenmeyer flasks, which were incubated at 26 °C for 10 days with an agitation rate of 250 rpm.

Extraction and Isolation. The mycelia cake from about 10 L fermentation broth was collected and extracted twice with acetone. The acetone solutions were combined and the solvents were evaporated under vacuum to give a crude oily extract. After addition of ~200 mL of Et_2O, the solids were removed by filtration. The filtrate was collected and concentrated to yield the crude yellow oil (~20 g) containing hygrocins A and B. The yellow oil was separated by preparative HPLC on an YMC ODS-A column (30 × 250 mm), and a gradient of H_2O/MeCN was used as the mobile phase (from 7:3 to 3.5:6.5 in 40 min at a flow rate of 20 mL/min). The peaks at 29.5 min (**2**) and 39.2 min (**1**) were collected into containers in an ice bath. After the solvents were evaporated, hygrocins A (**1**, 200 mg) and B (**2**, 98 mg) were obtained as yellow powders. Hygrocin A (**1**): $[\alpha]_D^{25}$ +19.91 (*c* 0.29, MeOH); IR (KBr) ν_{max} 3547, 3350, 2955, 1715, 1663, 1651, 1506, 1347 cm^{-1}; UV (MeOH/H_2O) λ_{max} (log ϵ) 275 (4.10), 316 (4.12) nm; ^{1}H and ^{13}C NMR data, see Table 1 and Table 2; EIMS *m/z* 510.2 $[M]^+$ (100); EIMS *m/z* 508.2 $[M]^-$ (100); HRMS *m/z* 510.2124 $[M]^+$ (calcd for $C_{28}H_{32}NO_8$ 510.2123). Hygrocin B (**2**): $[\alpha]_D^{25}$ +259.61 (*c* 0.21, MeOH); IR (KBr) ν_{max} 3432, 3289, 2961, 1740, 1665, 1627, 1578, 1341 cm^{-1}; UV (MeOH/H_2O) λ_{max} (log ϵ) 316 (4.21) nm; ^{1}H and ^{13}C NMR data, see Table 3; EIMS *m/z* 508.2 $[M]^+$ (100); EIMS *m/z* 506.2 $[M]^-$ (100); HRMS *m/z* 508.1960 $[M]^+$ (calcd for $C_{28}H_{30}NO_8$ 508.1965).

Diazomethane Derivative of Hygrocin A (3). Freshly prepared diazomethane reagent (2 mL in MeOH) was added to a 5 mL toluene solution containing 40 mg of **1** (0.078 mmol)

at 4 °C with stirring. This solution was gradually warmed to room temperature. After 2 h, the solvent was removed under vacuum to yield the crude products. The reaction product was purified by preparative HPLC on a HP/HPV column (50 × 300 mm, 7 μm). A gradient of water containing 5 mM of NH_4OAc/MeOH (from 6.5:3.5 to 1.5:8.5 in 60 min at a flow rate of 30 mL/min) was used as the mobile phase solvent system. The major product peak (t_R = 34 min) was collected. After solvents were removed under vacuum, 27 mg of the major diazomethane derivative **3** was obtained as a white powder: UV (MeOH/H_2O) λ_{max} (log ϵ) 267 (4.28), 302 (shd) nm; ^{1}H and ^{13}C NMR data, see Table 1 and Table 2; EIMS *m/z* 550.3 $[M]^-$ (100); HRMS *m/z* 552.2596 $[M]^+$ (calcd for $C_{31}H_{38}NO_8$ 552.2592). In the same way, the ^{13}C-labeled diazomethane derivative of hygrocin A was prepared: EIMS *m/z* 553.3 $[M]^-$ (100).

Alkaline Hydrolysis Product of Hygrocin A (4). NaOH (1 N, 0.8 mL) was added to a 1.2 mL solution of **1** (20 mg in 1:1 MeOH/H_2O) at room temperature with stirring. After 1 h, the reaction mixture was neutralized with 1 N HCl and subjected to isolation by preparative HPLC on a Zorbax RX-C18 column (21.2 × 250 mm, 10 μm). A gradient of H_2O/MeCN (from 8:2 to 3:7 in 40 min at a flow rate of 12 mL/min) was used as the mobile phase solvent system. The major product (t_R = 26.8 min) was collected. After the organic solvent was evaporated, the residue was lyophilized to yield 12 mg of hydrolytic product as a pale yellow powder, **4**: UV (MeOH/H_2O) λ_{max} (log ϵ) 276 (4.11), 316 (4.12) nm; ^{1}H and ^{13}C NMR data, see Table 1 and Table 2; EIMS *m/z* 400.2 $[M]^-$ (100).

Hydrogenation Product of Hygrocin A (5). 10% Pd/C (10 mg) was added to a 2 mL MeOH solution of **1** (10 mg) at room temperature. After stirring under H_2 for 2 h, the mixture was filtered through a syringe-filter to remove the catalyst. The filtrate was dried under vacuum to yield the crude hydrogenated product, which was purified by semipreparative HPLC on a semipreparative Supelcosil LC-18 column. A gradient of H_2O/MeCN (from 8:2 to 2:8 in 40 min at a flow rate of 4 mL/min) was used as the mobile phase solvent system. After evaporation of the solvent, about 5 mg of **5** was obtained as a white powder: UV (MeOH/H_2O) λ_{max} (log ϵ) 275 (4.10), 316 (4.12) nm; ^{1}H and ^{13}C NMR data, see Table 1 and Table 2; EIMS *m/z* 512.3 $[M]^-$ (100).

"Degradation" Product of Hygrocin A (6). From the recovered NMR solution of **1** (8 mg in 0.5 mL of DMSO-d_6), 4 mg of major "degradation" product was isolated by semipreparative HPLC as a pale yellow powder (**6**): UV (MeOH/H_2O) λ_{max} 275 (4.15), 306 (4.10) nm; ^{1}H and ^{13}C NMR data, see Table 1 and Table 2; EIMS *m/z* 508.3 $[M]^-$ (100).

Diazomethane Derivative of Hygrocin B (7). Freshly prepared diazomethane reagent (0.5 mL) was added to a 1 mL MeOH solution of **2** (10 mg) at 4 °C with stirring. This solution was gradually warmed to room temperature. After 2 h, the solvent was removed under vacuum to yield 8 mg of hygrocin B diazomethane derivative as a yellow powder (**7**): ^{1}H and ^{13}C NMR data, see Table 3; EIMS *m/z* 520.3 $[M]^-$ (100); HRMS *m/z* 522.2119 $[M]^+$ (calcd for $C_{29}H_{32}NO_8$ 522.2122).

Base Hydrolysis Product of Hygrocin B (8). NaOH (1 N, 0.2 mL) was added to a 0.6 mL solution of **2** (4 mg) in MeOH/H_2O (1:1) at room temperature with stirring. After 2 h, the reaction mixture was neutralized and extracted with EtOAc to yield product **8**: EIMS *m/z* 524.3 $[M]^-$ (100), 480 (20), 437 (65).

MTPA Esters 3s and 3r. To a 1 mL solution of **3** (3 mg) and DMAP (1 mg) in CH_2Cl_2 were added 8 μL of *R*-(−)-α-methoxy-α-(trifluoromethyl)phenylacetyl chloride (MTPA-Cl) and 20 μL of pyridine. The mixture was allowed to stir overnight at room temperature. After the solvent was evaporated under vacuum, the residue was purified by a small silica gel flash column to yield pure (*S*)-Mosher ester (**3s**, 1.6 mg). (*R*)-MTPA ester **3r** was prepared in the same manner using (*S*)-(+)-MTPA-Cl. **3s**: ^{1}H NMR (CD_3OD) δ 7.71 (1H, s, H-8), 7.25−7.40 (m, phenyl of MTPA), 5.664 (1H, bd, J = 2.4, 0.8 Hz, H-17), 5.517 (1H, dd, J = 16.2, 6.5 Hz, H-15), 5.404 (1H, dd, J = 16.2, 2.4 Hz, H-16), 5.239 (1H, bq, J = 6.5, 0.8 Hz, H-18), 3.89 (3H, s, C6-OCH_3), 3.44 (s, OCH_3 of MTPA), 2.42 (bd, H-21), 2.38 (1H, m, H-12), 2.23 (2H, bd, H-22), 1.69−1.74 (3H, m, H-12′, H-13a, H-13b), 1.58 (1H, m, H-14), 1.50 (2H, m, H-25), 1.174 (3H, d, H-27), 0.84 (3H, t, J = 7.0 Hz, H-26), 0.69 (3H, s, H-28), 0.52/1.10 and 0.06/0.42 (4H, cyclopropane protons). **3r**: ^{1}H NMR (CD_3OD) δ 7.71 (1H, s, H-8), 7.25−7.40 (m, phenyl of MTPA), 5.670 (1H, bd, J = 2.4, 0.8 Hz, H-17), 5.610 (1H, dd, J = 16.2, 6.5 Hz, H-15), 5.464 (1H, dd, J = 16.2, 2.4 Hz, H-16), 5.223 (1H, bq, J = 6.5, 0.8 Hz, H-18), 3.89 (3H, s, C6−OCH_3), 3.44 (s, OCH_3 of MTPA), 2.42 (bd, H-21), 2.38 (1H, m, H-12), 2.23 (2H, bd, H-22), 1.70−1.76 (3H, m, H-12′, H-13a, H-13b), 1.57 (1H, m, H-14), 1.50 (2H, m, H-25), 1.023 (3H, d, H-27), 0.85 (3H, t, J = 7.0 Hz, H-26), 0.72 (3H, s, H-28), 0.52/1.10 and 0.07/0.42 (4H, cyclopropane protons).

MTPA Esters 7s and 7r. These were prepared as described for compound **3s** and **3r**. From 3.3 mg and 4.0 mg of **7** were obtained 2.5 and 2.7 mg of (*S*)- and (*R*)-MTPA esters **7s** and **7r**. **7s**: EIMS *m/z* 738 $[M]^+$ (100); ^{1}H NMR (CD_3OD) δ 8.09 (1H, s, H-8), 7.47 (2H, m, phenyl), 7.25−7.16 (3H, m, phenyl), 6.13 (1H, d, J = 12.2 Hz, H-21), 6.00 (1H, d, J = 12.2 Hz, H-22), 5.651 (1H, dd, J = 16.0, 6.6 Hz, H-15), 5.141 (1H, bq, J = 6.5 Hz, H-18), 5.083 (1H, J = 16.0, 7.0 Hz, H-16), 3.76 (3H, s, 6-OCH_3), 3.519 (1H, bd, J = 7.0 Hz, H-17), 3.30 (3H, s, OCH_3 of MTPA), 2.48 (2H, m, H-12), 2.46 (3H, s, 7-CH_3), 2.01 (1H, m, H-13a), 1.58 (1H, m, H-14), 1.56 (3H, s, H-28), 1.36 (3H, m, H-13b and H-25), 1.233 (3H, d, H-27), 0.86 (3H, t, J = 7.0 Hz, H-26). **7r**: EIMS *m/z* 738 $[M]^+$ (100); ^{1}H NMR (CD_3OD) δ 8.09 (1H, s, H-8), 7.47 (2H, m, phenyl), 7.25−7.16 (3H, m, phenyl), 6.12 (1H, d, J = 12.2 Hz, H-21), 5.99 (1H, d, J = 12.2 Hz, H-22), 5.662 (1H, dd, J = 16.0, 6.6 Hz, H-15), 5.241 (1H, J = 16.0, 7.0 Hz, H-16), 5.125 (1H, bq, J = 6.5 Hz, H-18), 3.78 (3H, s, C6−OCH_3), 3.521 (1H, bd, J = 7.0 Hz, H-17), 3.29 (3H, s, OCH_3 of MTPA), 2.48 (2H, m, H-12), 2.46 (3H, s, 7-CH_3), 2.01 (1H, m, H-13a), 1.58 (1H, m, H-14), 1.56 (3H, s, H-28), 1.36 (3H, m, H-13b and H-25), 1.126 (3H, d, H-27), 0.84 (3H, t, J = 7.0 Hz, H-26).

Acknowledgment. The authors thank X. Feng for obtaining the high-resolution MS data and Y. Gong for collecting some NMR data.

References and Notes

(1) Sehgal, S. N.; Baker, H.; Vezinna, C. *J. Antibiot.* **1975**, *28*, 727−732.
(2) Streinrauf, L. K. *Biochem. Biophys. Res. Commun*. **1968**, *33*, 29−32.
(3) Gerlitz, M.; Hammann, P.; Thiericke, R.; Rohr, J. *J. Org. Chem.* **1992**, *57*, 4030−4033.
(4) Furumai, T.; Yamakawa, T.; Yoshida, R.; Igarashi, Y. *J. Antibiot.* **2003**, *56*, 700−708.
(5) March, J. In *Advaced Organic Chemistr: Reactions, Mechanisms and Structure;* John Wiley & Son: New York, 1985; pp 174−175.
(6) Ohtani, I.; Kusumi, T.; Kashman, Y.; Kakisawa, H. *J. Am. Chem. Soc*. **1991**, *113*, 4092−4096.
(7) Whitfield, G. B.; Olson, E. C.; Herr, R. R.; Fox, J. A.; Bergy, M. E.; Boyack, G. A. *Am. Rev. Tuberc. Pulm. Dis.* **1957**, *75*, 584−588.
(8) Kim, J. S.; Shin-ya, K.; Eishima, J.; Furihata, K.; Seto. *J. Antibiot*. **1996**, *49*, 1172−1173.
(9) Meyer, M.; W. Keller-Schierlein, W.; Megahed, S.; Zaehner, H.; Segre, A. *Helv. Chim. Acta* **1986**, *69*, 1356−1364.
(10) Schupp, T.; Traxler, P.; Auden, J. A. L. *J. Antibiot.* **1981**, *34*, 965−970.
(11) Startmann, A.; Schupp, T.; Toupet, C.; Schilling, W.; Oberer, L.; Traber, R. *J. Antibiot.* **2002**, *55*, 396−406.
(12) (a) The in vitro antibacterial activities of **1** and **2** were tested using the National Committee for Clinical Laboratory Standard M-27A Procedure. (b) Traxler, P.; Schupp, T.; Fuhrer, H.; Richter, W. J. *J. Antibiot*. **1981**, *34*, 971−979. (c) Kasik, J. E.; Monick, M. *Antimicrob. Agents Chemother.* **1981**, *19*, 134−138.

NP050272L